



# Drug Binding Poses Relate Structure with Efficacy in the $\mu$ Opioid Receptor

Katy J. Sutcliffe<sup>1,2</sup>, Graeme Henderson<sup>1</sup>, Eamonn Kelly<sup>1</sup> and Richard B. Sessions<sup>2</sup>

<sup>1</sup> - School of Physiology, Pharmacology and Neuroscience, University of Bristol, Bristol BS8 1TD, UK

<sup>2</sup> - School of Biochemistry, University of Bristol, Bristol BS8 1TD, UK

**Correspondence to Katy J. Sutcliffe:** School of Physiology, Pharmacology & Neuroscience, Faculty of Biomedical Sciences, Biomedical Sciences Building, University of Bristol, Bristol, BS8 1TD, UK. [katy.sutcliffe@bristol.ac.uk](mailto:katy.sutcliffe@bristol.ac.uk)

<http://dx.doi.org/10.1016/j.jmb.2017.05.009>

Edited by Patrick Griffin

## Abstract

The  $\mu$ -opioid receptor (MOPr) is a clinically important G protein-coupled receptor that couples to  $G_{i/o}$  proteins and arrestins. At present, the receptor conformational changes that occur following agonist binding and activation are poorly understood. This study has employed molecular dynamics simulations to investigate the binding mode and receptor conformational changes induced by structurally similar opioid ligands of widely differing intrinsic agonist efficacy, norbuprenorphine, buprenorphine, and diprenorphine. Bioluminescence resonance energy transfer assays for  $G_i$  activation and arrestin-3 recruitment in human embryonic kidney 293 cells confirmed that norbuprenorphine is a high efficacy agonist, buprenorphine a low efficacy agonist, and diprenorphine an antagonist at the MOPr. Molecular dynamics simulations revealed that these ligands adopt distinct binding poses and engage different subsets of residues, despite sharing a common morphinan scaffold. Notably, norbuprenorphine interacted with sodium ion-coordinating residues W293<sup>6,48</sup> and N150<sup>3,35</sup>, whilst buprenorphine and diprenorphine did not. Principal component analysis of the movements of the receptor transmembrane domains showed that the buprenorphine-bound receptor occupied a distinct set of conformations to the norbuprenorphine-bound receptor. Addition of an allosteric sodium ion caused the receptor and ligand to adopt an inactive conformation. The differences in ligand–residue interactions and receptor conformations observed here may underlie the differing efficacies for cellular signalling outputs for these ligands.

© 2017 The Authors. Published by Elsevier Ltd. This is an open access article under the CC BY license (<http://creativecommons.org/licenses/by/4.0/>).

## Introduction

The  $\mu$ -opioid receptor (MOPr) is a  $G_{i/o}$  coupled receptor from the class A G protein-coupled receptor (GPCR) family. It is responsible for both the analgesic and euphoric effects of many opioid drugs [1] and is therefore a protein of very significant clinical and societal importance.

The process of GPCR activation, and particularly the molecular difference between high and low efficacy agonists, is poorly understood. The current consensus is that ligand binding induces changes in residue orientation around the ligand binding pocket, termed micro-switches, that translate to larger rearrangements of the intracellular regions of the receptor, hence promoting engagement with intracellular sig-

nalling partners such as G proteins and arrestins [2,3]. One well-established hallmark of receptor activation is the outward movement of the lower part of transmembrane domain (TM) 6 and the concurrent small inward shifts of TM5 and TM7, thus opening an intracellular cavity in the receptor into which G protein or arrestin can bind [4–9].

Residues forming a conserved network of polar interactions allosterically connecting the ligand binding site and the intracellular face of MOPr [9–11] also include those that comprise an allosteric sodium ion binding site [12]. Sodium has been previously described as a negative allosteric modulator of MOPr and other class A GPCRs [13–18], and a high-resolution X-ray crystal structure of the  $\delta$ -opioid receptor bound to an antagonist revealed a sodium

challenge; however, in 2022 this might be a solved challenge.

ion coordinated by conserved residues below the ligand binding pocket [19]. These residues have been proposed to be involved in signal transmission from the ligand binding pocket to the G protein binding site [11,20–23]. However, there is limited understanding of the precise nature of this signal transmission through the protein and hence the molecular nature of agonist efficacy.

The MOPr ligands norbuprenorphine, buprenorphine, and diprenorphine share the same morphinan scaffold (Fig. 1a), and all exhibit affinities for MOPr in the nanomolar range [24,25] yet display fundamental differences in intrinsic efficacy. Norbuprenorphine, a metabolite of buprenorphine [26], is a full agonist at MOPr, able to activate G proteins and recruit arrestin-3, whilst buprenorphine is a MOPr partial agonist, producing a submaximal activation of G protein, and is unable to induce measurable arrestin-3 recruitment to the receptor [27]. Diprenorphine is a MOPr antagonist [24], that is, it has extremely low or zero efficacy. In this study, we first confirmed the signalling characteristics of these ligands using bioluminescence resonance energy transfer (BRET) assays. Then, these structurally related ligands were used in molecular dynamics (MD) simulations of MOPr to explore ligand binding

poses, residue interactions, and MOPr conformations, which may confer the different abilities of these ligands to engage intracellular signalling partners.

## Results

### Agonist-induced G protein activation and arrestin-3 recruitment

Human embryonic kidney 293 (HEK 293) cells expressing HA-tagged rat MOPr, *Gai*-renilla luciferase (Rluc) II, and G $\beta\gamma$ -green fluorescent protein (GFP) were used to detect dissociation of the G $\alpha$  and G $\beta\gamma$  subunits upon activation. A decrease in the BRET ratio compared to cells treated with media or 0.01% DMSO alone indicated dissociation, or rearrangement, of these subunits [28]. HEK 293 cells expressing rat MOPr-yellow fluorescent protein (YFP) and arrestin-3-Rluc were used to detect ligand-induced recruitment of arrestin-3 to MOPr. An increase in this BRET ratio indicates arrestin-3 and MOPr coming into closer proximity [29]. Concentration-response curves for G $_i$  activation and arrestin-3 recruitment by the MOPr ligands compared to the standard full agonist DAMGO

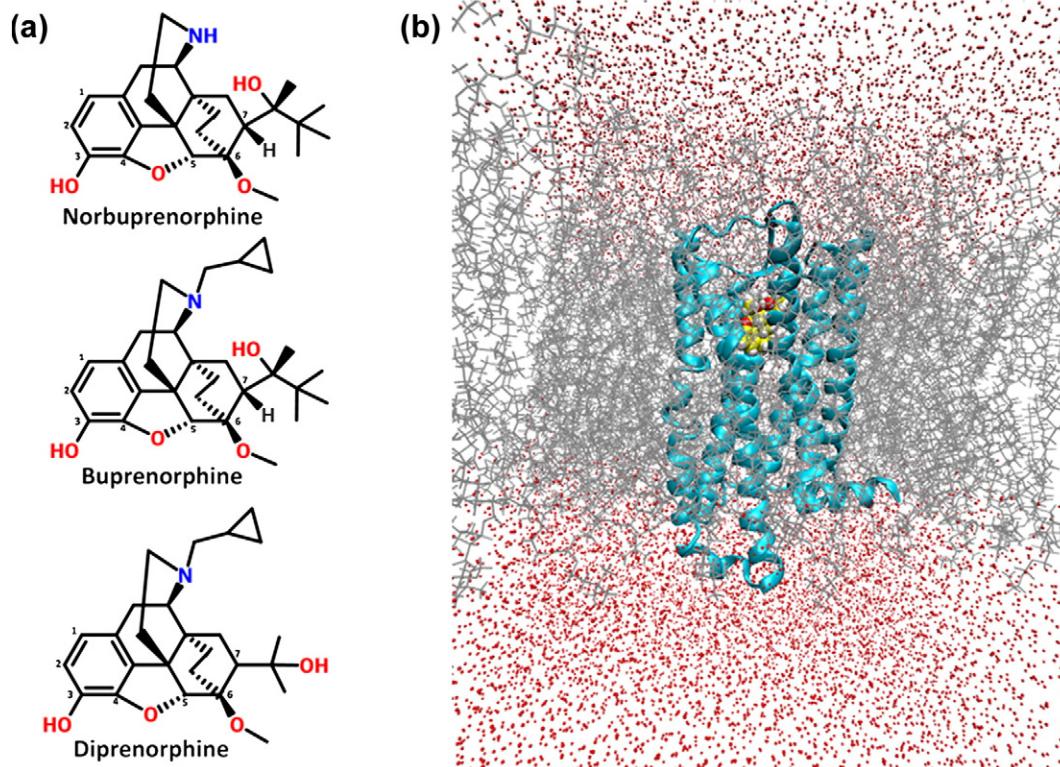


**Fig. 1.** Structurally similar ligands were used in MD simulations bound to MOPr. (a) Structures of the MOPr ligands used in this study, sharing the same morphinan scaffold. Carbons 1–7 are labelled. (b) Model of MOPr (cyan) bound to a ligand, norbuprenorphine (yellow), and embedded in a cholesterol and phospholipid bilayer (grey) solvated in water and NaCl (red), developed from the antagonist-bound crystal structure [31].

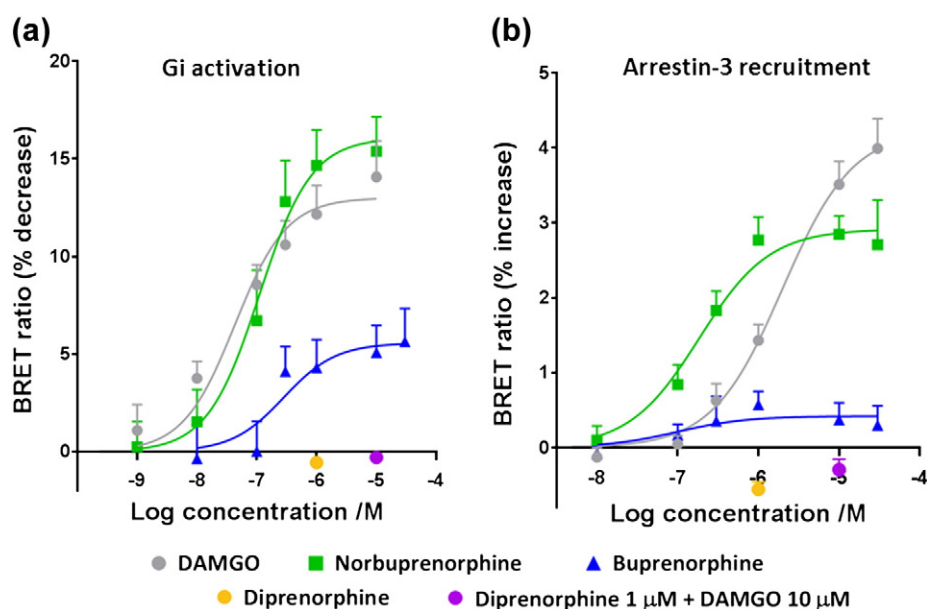


**Fig. 2.** MOPr ligand concentration-response curves from BRET assays. Data obtained by BRET assay in HEK 293 cells (see Materials and Methods) for (a)  $G_i$  activation and (b) arrestin-3 recruitment to MOPr. Values are mean  $\pm$  SEM for 3–6 independent experiments.

are shown in Fig. 2.  $EC_{50}$  and maximum response values for each agonist are listed in Table 1. Compared to DAMGO, norbuprenorphine was a full agonist for  $G_i$  activation (Fig. 2a) and a potent partial agonist for arrestin-3 recruitment (Fig. 2b), producing approximately 70% of the maximum DAMGO response (Table 1). Norbuprenorphine displayed approximately 10-fold higher potency than DAMGO in the arrestin-3 recruitment and a similar potency as DAMGO for  $G_i$  activation (Table 1). Buprenorphine was a weak partial agonist for  $G_i$  activation, producing less than 50% of the maximum response achieved by DAMGO (Fig. 2a). Buprenorphine produced very little response in the arrestin-3 recruitment assay (Fig. 2b). A high concentration (1  $\mu$ M) of diprenorphine did not produce a response in the  $G_i$  activation (Fig. 2a) or arrestin-3 recruitment assays (Fig. 2b). Incubation of cells with 1  $\mu$ M diprenorphine for 10 min prior to the addition of 10  $\mu$ M DAMGO completely inhibited the DAMGO response for both  $G_i$  activation and arrestin-3 recruit-

ment (Fig. 2), confirming that diprenorphine is a MOPr antagonist, with extremely low or zero efficacy.

### Ligand binding poses and residue interactions

Both conventional MD (cMD) and accelerated MD (aMD) simulations were conducted with murine MOPr (Fig. S6) embedded in a phospholipid and cholesterol bilayer as described in Materials and Methods (Fig. 1b) and bound to norbuprenorphine, buprenorphine, or diprenorphine. aMD is a method of increasing sampling over a short computational time by employing a boost potential to accelerate conformational changes [30]. Moreover, 8 repeats of 125-ns long simulations were performed (with different initial velocities) for each ligand–receptor pair with each method, giving a total of 6  $\mu$ s of trajectory data. The structure of antagonist  $\beta$ -funaltrexamine ( $\beta$ -FNA) bound to MOPr was used as a template to decide the initial orientation of these

**Table 1.**  $EC_{50}$  and maximum response values for MOPr ligands in the BRET assay in HEK 293 cells

| Ligand           | $G_i$ activation       |                               | Arrestin-3 recruitment |                               |
|------------------|------------------------|-------------------------------|------------------------|-------------------------------|
|                  | $EC_{50} \pm$ SEM (nM) | $E_{max}$ (relative to DAMGO) | $EC_{50} \pm$ SEM (nM) | $E_{max}$ (relative to DAMGO) |
| DAMGO            | 42.9 $\pm$ 16.9        | 1.0 $\pm$ 0.07                | 1980 $\pm$ 473         | 1.0 $\pm$ 0.06                |
| Norbuprenorphine | 110 $\pm$ 44.9         | 1.23 $\pm$ 0.12               | 184 $\pm$ 64.5         | 0.69 $\pm$ 0.05               |
| Buprenorphine    | 283 $\pm$ 232          | 0.43 $\pm$ 0.08               | – *                    | 0.10 $\pm$ 0.03               |

Data are mean  $\pm$  SEM for 4–6 independent experiments. Maximum response is expressed relative to DAMGO. \*  $EC_{50}$  value in the arrestin recruitment assay for buprenorphine was approximately 100 nM.

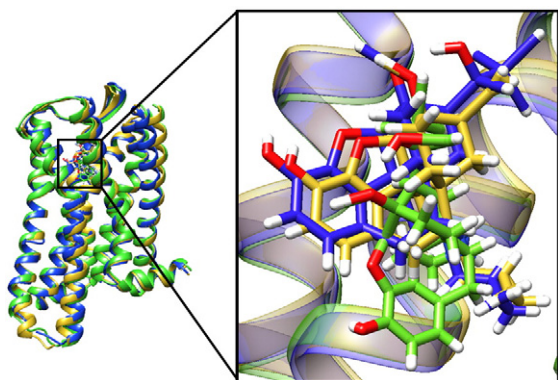


**Fig. 3.** Ligands have different binding poses. Overlay of the average binding poses of MOPr ligands from 1  $\mu$ s of accelerated MD simulations. Buprenorphine (blue) and diprenorphine (yellow) adopt a position higher in the binding pocket than norbuprenorphine (green).

ligands [31]. Figures 3 and S1 show the average binding poses after 1  $\mu$ s of aMD. Despite sharing a common morphinan scaffold and being docked into the same initial binding position, norbuprenorphine adopted a different binding pose to buprenorphine and diprenorphine within the ligand binding pocket. The amine–D147<sup>3,32</sup> hydrogen bond is essential for opioid binding [32] (superscript numbers follow the Ballesteros–Weinstein numbering system for GPCR residues [33]). Ligands pivoted about this interaction, with norbuprenorphine favouring a position lower (i.e., closer to the intracellular side) in the binding pocket compared to the lower efficacy ligands (Fig. 4). The presence of the cyclopropylmethyl group (Fig. 1a) restricted the ability of buprenorphine and diprenorphine to pivot about the amine–D147<sup>3,32</sup> interaction; therefore, these ligands favoured a position higher (i.e., nearer to the extracellular side) in the binding pocket. These binding poses were consistent across both 1  $\mu$ s of cMD and 1  $\mu$ s of aMD; RMSD plots comparing each ligand to its average binding position show that none of the ligands deviated from the presented average binding pose by more than 1 Å (Fig. S3), and these

average binding positions were similar between the aMD and cMD simulations (Fig. S4).

Distances between the heavy atoms of the bound ligand and the residues comprising the binding pocket (Fig. S2) were recorded over the 1- $\mu$ s simulation time. Residues within 4 Å of each ligand, measured from the average structures, are compared in Table 2, whilst Fig. S5 shows the percentage of simulation time that each residue is within this 4-Å cut-off distance. The MOPr ligands shared some residue interactions; for instance, all three ligands were in contact with D147<sup>3,32</sup> for at least 80% of the simulation time in both cMD and aMD (Fig. S5) and interacted with H297<sup>6,52</sup>; both residues are known to be essential for opioid ligand binding [32,34]. In both the aMD and cMD simulations, buprenorphine and diprenorphine were able to interact with K233<sup>5,39</sup>, V236<sup>5,42</sup>, V300<sup>6,55</sup>, and W318<sup>7,35</sup>, due to their location higher in the binding pocket, whilst norbuprenorphine adopted a position further away from these side chains. Similarly, buprenorphine makes contact with Q124<sup>2,60</sup> and I144<sup>3,29</sup> due to the carbon-7 side chain (refer to Fig. 1a), whilst diprenorphine lacks this carbon-7 group, and norbuprenorphine sits too low in the receptor binding pocket. Overall, buprenorphine participated in a greater number of ligand–residue interactions in both the aMD and cMD simulations than norbuprenorphine or diprenorphine, which may contribute to the slow dissociation rate of this ligand, compared to norbuprenorphine and diprenorphine [35]. These ligand–residue interactions are similar for both aMD and cMD simulations (Table 2). Differences between the two techniques likely reflect the enhanced sampling by aMD and do not affect the overall interpretation.

It is noteworthy that the high efficacy agonist norbuprenorphine interacted with W293<sup>6,48</sup> and W293 is key to high or low efficacy. whilst the low efficacy agonist and the antagonist did not. Closer inspection of the simulation trajectories revealed that this is due to a small rotation of TM3, causing the N150<sup>3,35</sup> side chain to fall out of the 4-Å range for buprenorphine and diprenorphine

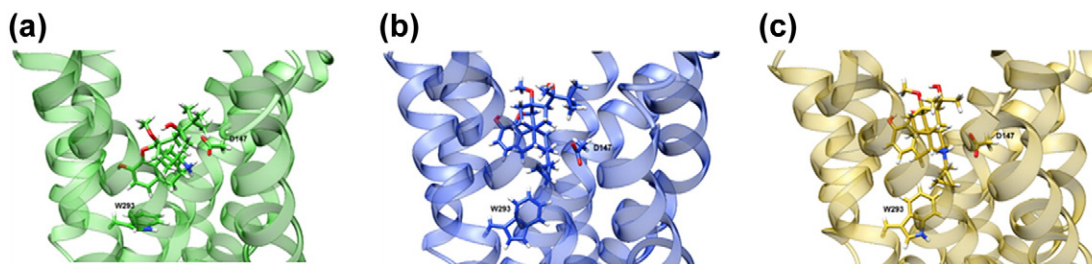


**Fig. 4.** Conformation of the W293<sup>6,48</sup> toggle switch. Representative snapshots of (a) the norbuprenorphine-bound receptor, (b) buprenorphine-bound receptor, and (c) diprenorphine-bound receptor. Showing the ligand, essential residue for opioid binding D147<sup>3,32</sup>, and the different conformations of the conserved W293<sup>6,48</sup> rotamer toggle switch.

def not the best color scheme to illustrate the sidechain interaction. can barely see the residues clearly.

**Table 2.** Ligand–residue interactions

| (a)              |   | Q124 | I144 | D147 | Y148 | N150 | M151 | K233 | V236 | W293 | I296 | H297 | V300 | W318 | I322 | G325 | Y326 |
|------------------|---|------|------|------|------|------|------|------|------|------|------|------|------|------|------|------|------|
| Accelerated MD   |   |      |      |      |      |      |      |      |      |      |      |      |      |      |      |      |      |
| Norbuprenorphine |   |      |      | ■    | ■    | ■    | ■    |      |      | ■    | ■    | ■    |      |      | ■    | ■    | ■    |
| Buprenorphine    | ■ | ■    | ■    | ■    |      |      | ■    | ■    | ■    |      | ■    | ■    | ■    | ■    | ■    | ■    | ■    |
| Diprenorphine    |   |      | ■    | ■    |      |      | ■    | ■    | ■    |      | ■    | ■    | ■    | ■    | ■    | ■    | ■    |

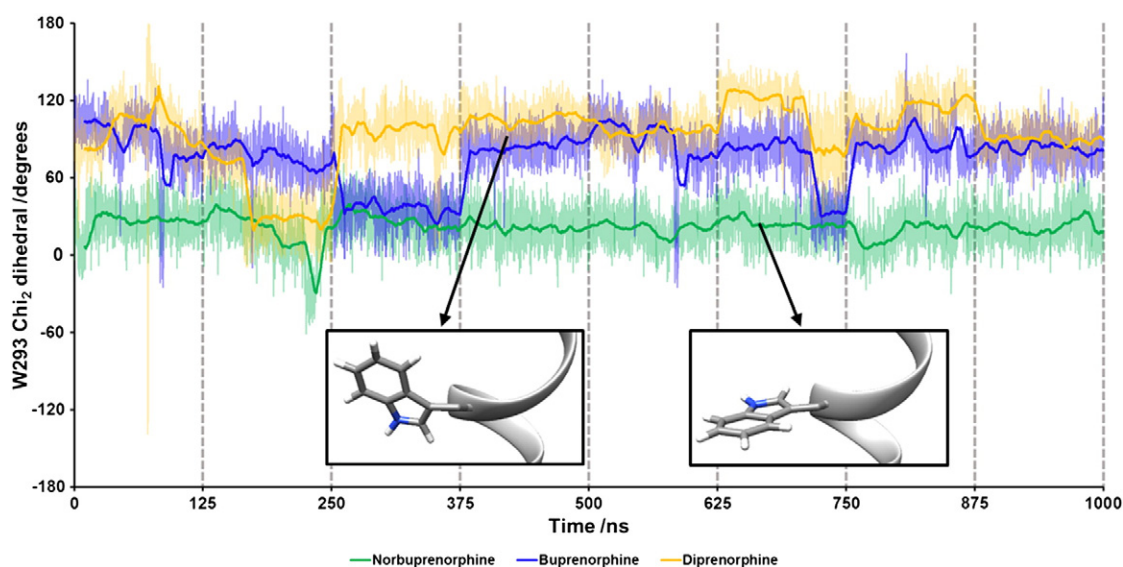
  

| (b)              |   | Q124 | I144 | D147 | Y148 | N150 | M151 | K233 | V236 | W293 | I296 | H297 | V300 | W318 | I322 | G325 | Y326 |
|------------------|---|------|------|------|------|------|------|------|------|------|------|------|------|------|------|------|------|
| Conventional MD  |   |      |      |      |      |      |      |      |      |      |      |      |      |      |      |      |      |
| Norbuprenorphine | ■ |      | ■    | ■    |      |      | ■    |      |      | ■    | ■    | ■    | ■    | ■    | ■    | ■    | ■    |
| Buprenorphine    |   | ■    | ■    | ■    |      |      | ■    | ■    | ■    |      | ■    | ■    | ■    | ■    | ■    | ■    | ■    |
| Diprenorphine    |   |      | ■    | ■    |      |      | ■    | ■    | ■    |      | ■    | ■    | ■    | ■    | ■    | ■    | ■    |

Residues within 4 Å of the bound ligand, measured from the average structure of 1- $\mu$ s simulation data in each case. (a) Accelerated MD; (b) conventional MD.

interaction, whilst W293<sup>6.48</sup> undergoes significant changes in the angle of its side chain (Fig. 4). These rotamer changes can be monitored by plotting the  $\chi_2$  angle, as shown for the cMD simulation in Fig. 5.

With norbuprenorphine bound, the indole ring of W293<sup>6.48</sup> favours a “horizontal” conformation, parallel to the lipid bilayer, maintaining a  $\chi_2$  angle of 0–60°, and spanning the base of the ligand binding site.



**Fig. 5.** Rotamer angle of W293<sup>6.48</sup> with each ligand bound, during 1  $\mu$ s of conventional MD simulations. With norbuprenorphine bound, W293<sup>6.48</sup> favours a horizontal conformation. Each dataset is plotted as raw data and a running average (solid lines).

This orientation obstructs the allosteric sodium ion site (Figs. 4a and 5). With buprenorphine (Figs. 4b and 5) or diprenorphine bound (Figs. 4c and 5), the side chain of W293<sup>6,48</sup> adopts a “vertical” conformation, with the indole ring of the tryptophan perpendicular to the bilayer, favouring a  $\chi_2$  angle between 80 and 120° and pointing into the ligand binding pocket. Both buprenorphine- and diprenorphine-bound receptors occasionally sample the “horizontal” conformation of W293<sup>6,48</sup>, with buprenorphine more frequently than diprenorphine (Fig. 5).

### Principal component analysis shows distinct helical arrangements

Large, high-dimensional datasets, such as that obtained by MD, are difficult to analyse by eye or simple statistics. Principal component (PC) analysis (PCA) is a method of reducing highly dimensional data to the main “principal components”, which account for the most variation [36]. PCA was used in this study to plot subtle changes in receptor conformation and allow the mapping of clusters of conformations explored by the different receptor–ligand complexes. After aligning all trajectories to a set of “core residues” that showed the least movement over the simulation time (Fig. S6a), PCA was performed on the three-dimensional Cartesian coordinates of the alpha carbons of the receptor TMs (Fig. S6b) to avoid variations being masked by the highly dynamic extracellular and intracellular loops and side-chain movements. The receptor conformation at each time point was projected onto PCs 1 and 2, producing clusters of receptor conformations that converge if the helical structures are

becoming more similar or diverge if the conformations are different. For the cMD simulations, PCs 1 and 2 account for 28.2% and 11.3% of the variance, respectively. For the aMD, PCs 1 and 2 account for 14.2% and 9.7% of the variance. In both the aMD (Fig. 6a) and cMD (Fig. 6b), the norbuprenorphine-bound MOPr and buprenorphine-bound MOPr form distinct clusters. This indicates different helical arrangements depending on the bound ligand. An overlay of structures extracted from the norbuprenorphine-bound cluster and the buprenorphine-bound cluster is shown in Fig. S7. There are multiple shifts in the positions of several of the transmembrane helices, notably the movement of the extracellular ends of TM1, 2 and 3, and the intracellular end of TM5. The diprenorphine-bound MOPr cluster overlaps somewhat with the buprenorphine-bound cluster, suggesting that the buprenorphine-bound receptor favours a more inactive conformation compared with the norbuprenorphine-bound receptor. The greater spread of the aMD PCA plot (Fig. 6a) shows that the conformational space sampled by aMD is greater than that by the cMD simulations (Fig. 6b), highlighting the value of this technique in increasing sampling over relatively short computational time. Nevertheless, both approaches gave the same overall result.

### Effect of an allosteric sodium ion on ligand binding pose and W293<sup>6,48</sup> conformation

During unliganded MOPr simulations, a sodium ion was observed to move from the extracellular space into the receptor pore to occupy the allosteric sodium site (data not shown). The coordinates of this sodium ion were used to set up two repeats of 125-ns cMD

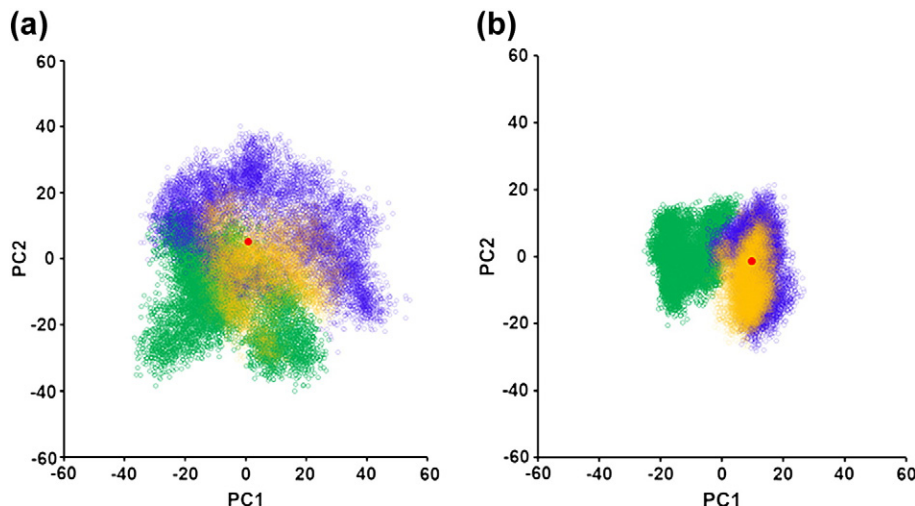
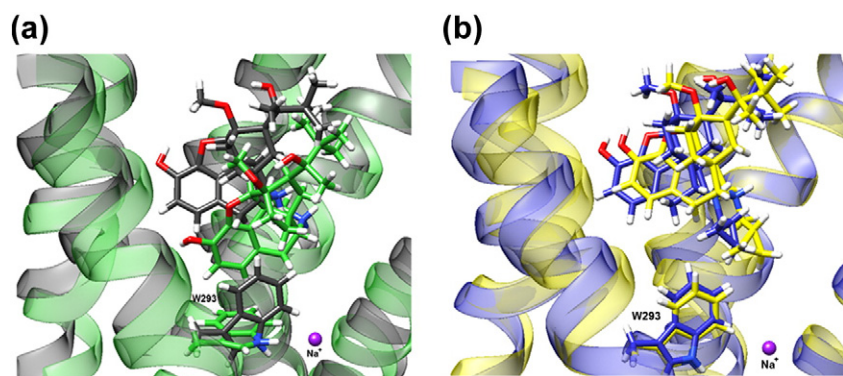


**Fig. 6.** Principal component analysis shows distinct receptor–ligand clusters. Projection of the receptor conformation at each time point onto principal components 1 and 2 (see Materials and Methods). (a) Accelerated MD and (b) conventional MD simulations. The norbuprenorphine-bound receptor is in green, buprenorphine-bound receptor in blue, and diprenorphine-bound receptor in yellow. The conformation of the crystallised  $\beta$ -FNA-bound receptor is projected in red.



side chain points upwards (dark grey). The binding pose of buprenorphine and the preferred angle of the W293<sup>6.48</sup> side chain in the absence (blue) and presence (yellow) of sodium do not differ.

and aMD simulations of MOPr bound to norbuprenorphine or buprenorphine in the presence of an allosteric sodium ion, giving a total of 1  $\mu$ s of trajectory data. Ligand binding poses and the conformation of the W293<sup>6.48</sup> rotamer in the presence and absence of an allosteric sodium ion are shown in Fig. 7. These conformations were consistent between cMD and aMD simulations. The sodium ion did not leave the allosteric site during the simulation time for either cMD or aMD for either ligand. In the norbuprenorphine-bound simulations (Fig. 7a), the presence of a sodium ion caused the ligand to shift upwards in the binding pocket to occupy a position similar to buprenorphine and diprenorphine. The rotamer of W293<sup>6.48</sup> switched from a horizontal conformation to the vertical conformation favoured by the buprenorphine- and

diprenorphine-bound receptor, pointing into the ligand binding pocket. In the buprenorphine-bound simulations (Fig. 7b), the presence of a sodium ion did not induce significant change in the ligand binding pose or the W293<sup>6.48</sup> rotamer. The  $\chi^2$  angle for W293<sup>6.48</sup> in the presence or absence of sodium for each ligand bound simulation is plotted in Fig. S8. In the presence of sodium, the W293<sup>6.48</sup>  $\chi^2$  angle of norbuprenorphine-bound MOPr is maintained at around 80–120°, comparable to the buprenorphine-bound MOPr in both the presence and absence of sodium. RMSD plots indicate that these ligand binding poses in the presence of an allosteric sodium were stable for the entirety of the simulation time (Fig. S9).

PCA was performed on the receptor TMs as described above. With the sodium ion present, both

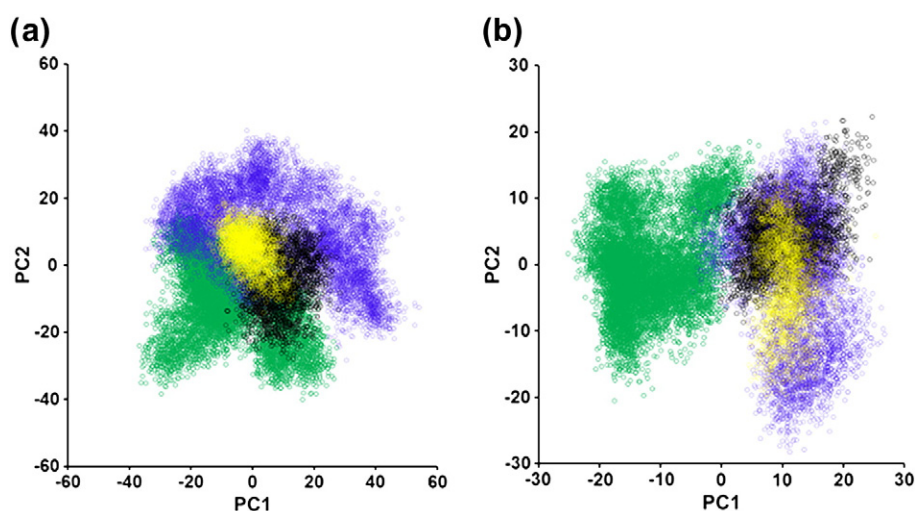


**Fig. 8.** Principal component analysis in the absence and presence of an allosteric sodium ion. Projection of the receptor conformation at each time point onto principal components 1 and 2 (see Materials and Methods). (a) Accelerated MD and (b) conventional MD simulations. The norbuprenorphine-bound receptor in the absence of an allosteric sodium is in green and buprenorphine-bound receptor in the absence of sodium in blue. The norbuprenorphine-bound receptor in the presence of sodium is in black, and the buprenorphine-bound receptor in the presence of sodium is in yellow.

the buprenorphine and norbuprenorphine clusters overlap with the sodium-free buprenorphine-bound cluster (Fig. 8) and the diprenorphine-bound cluster (Fig. 6). This is consistent for both aMD (Fig. 8a) and cMD simulations (Fig. 8b). Taken together, these PCA plots and the change in ligand binding pose and rotamer of W293<sup>6,48</sup> suggest that the presence of an allosteric sodium ion causes the norbuprenorphine-bound MOPr to favour an inactive conformation, whilst the buprenorphine-bound MOPr is relatively unchanged.

## Discussion

The results from the BRET assay confirm previous studies characterising norbuprenorphine as a high efficacy agonist capable of recruiting arrestin-3 to MOPr, buprenorphine as a low efficacy agonist with minimal or no arrestin recruitment to the receptor, and diprenorphine as an antagonist for G protein activation and arrestin-3 recruitment, with very low or zero efficacy [24,27]. Based on some previous studies [27], buprenorphine would be expected to have higher potency in the G protein activation assay; however, higher than expected EC<sub>50</sub> values for buprenorphine in signalling assays have been reported by others [37]. When compared to the balanced agonist DAMGO, norbuprenorphine appears to display a degree of arrestin bias in these assays. McPherson *et al.* [27] did not report norbuprenorphine exhibiting significant bias between GTP $\gamma$ S binding and arrestin PathHunter assays. This discrepancy may be due to the different assay systems used or that norbuprenorphine could be an arrestin-biased agonist and will be the subject of further investigation.

Both cMD and aMD simulations revealed that these structurally similar ligands adopted distinct binding positions in the ligand binding pocket. The simulated binding poses were maintained over the entire simulation time. Each 125-ns repeat simulation was started from a newly minimised structure and the dynamics initialised with new random velocities and the standard heating protocol. Furthermore, the ligand binding poses for each ligand were similar between repeats of cMD and aMD simulations, giving confidence that the sampling was adequate and the differences in poses seen for the different ligands may be relevant to the physiological situation. Recently reported MD simulations of the  $\beta_2$  adrenoceptor revealed ligand–protein interaction fingerprints for a variety of different ligands that correlated with the drug efficacy and the size of the intracellular G protein binding cavity, although the binding positions of the ligands were not greatly different [38].

The presence of a cyclopropylmethyl group on the amine confers a degree of antagonist activity in

MOPr ligands [18,39,40]. In our simulations, this shared N substituent in buprenorphine and diprenorphine appeared to reduce the ability of the ligand to pivot about the amine–D147<sup>3,32</sup> interaction so that these low efficacy ligands sat higher in the binding pocket and did not interact with residues in the sodium ion allosteric site and conserved polar network. Using MD simulations of the agonist-bound MOPr, Huang *et al.* [6] have shown that the binding pose of the antagonist BU74 is unstable when the cyclopropylmethyl group was docked into the polar cavity at the base of the binding site and shifts upwards in the binding pocket, suggesting that this ring group cannot stably interact with residues in this polar cavity and in agreement with the data we present here.

The residue W293<sup>6,48</sup> has previously been identified as a rotamer toggle switch for GPCR activation in the conserved polar network and participating in coordination of a sodium ion [6,41–45]. The MD simulations described here showed that the full agonist norbuprenorphine came into close contact with this residue, affecting the preferred rotamer of the W293<sup>6,48</sup> side chain, whereas the low efficacy agonist buprenorphine and antagonist diprenorphine did not. This provides an explanation for the differing efficacies of these ligands. Norbuprenorphine is able to activate this rotamer toggle switch, thus disrupting the allosteric sodium site and allowing MOPr to adopt an active conformation. Buprenorphine and diprenorphine are less able to alter the W293<sup>6,48</sup> rotamer, so MOPr is less likely to adopt an active conformation. Both the MOPr crystallised with agonist BU72 and the recently described G protein-biased agonist PZM21 also appear to interact with W293<sup>6,48</sup> [6,46]. Moreover, MD simulations of MOPr bound to BU72 or another agonist  $\beta$ -fuoxymorphanine show changes in the W293<sup>6,48</sup> rotamer, suggesting that interaction with this residue is a common mechanism amongst small molecule MOPr agonists [6]. However, these MD simulations with BU72 show the opposite conformation of the W293<sup>6,48</sup> rotamer to that described here, whilst the  $\chi_2$  angle of this residue in MD simulations with hydromorphanine or morphine bound was different again [47]. This alternative behaviour of W293<sup>6,48</sup> in the presence of different ligands indicates that receptor activation involves a complex mechanism to give rise to the different helix conformations observed in the present study and cannot be simply explained by a single key residue.

Buprenorphine is a low efficacy agonist [24,25] but is able to activate MOPr, albeit producing a lower maximum response than higher efficacy agonists. The MD simulations reported here showed buprenorphine adopting an overlapping binding pose, partially overlying PCA clusters, and a similar W293<sup>6,48</sup> rotamer to the antagonist diprenorphine. This poses the question of how buprenorphine activates MOPr;

so there is a discrepancy or a dispute going on.



one possibility is that buprenorphine is sometimes able to engage the W293<sup>6,48</sup> toggle switch but with lower probability than the high efficacy agonist norbuprenorphine. Indeed, during these MD simulations, buprenorphine did infrequently alter its binding position to overlap with the norbuprenorphine binding pose, with a corresponding change in W293<sup>6,48</sup> rotamer (Fig. 5). Another possibility is that buprenorphine is capable of activating MOPr via an alternative mechanism than the W293<sup>6,48</sup> rotamer. An NMR study of MOPr in the presence and absence of BU72 showed initial agonist-induced conformational changes in helix 8 and intracellular loop 1 preceding the larger movements of TM5 and TM6 [7], although the mechanism of ligand-induced changes in helix 8 and intracellular loop 1 is not yet known. Recently, an MD study comparing MOPr bound to morphine and the G protein-biased ligand TRV-130 revealed alternative allosteric transduction mechanisms between the ligand binding pocket and intracellular G protein binding site for these two drugs [48]. It is possible that buprenorphine can also produce receptor activation via a different mechanism. The PCA plots show the buprenorphine-bound MOPr occupying conformations distinct from both the norbuprenorphine- and diprenorphine-bound receptors (Fig. 6). This may represent a different active conformation stabilised by buprenorphine.

If norbuprenorphine-bound MOPr favours an active conformation, we would predict that the presence of the negative allosteric modulator, sodium, would disrupt this conformation. Indeed, we found that whilst an allosteric sodium ion did not significantly alter the binding pose, W293<sup>6,48</sup> rotamer, and PCA clustering of the buprenorphine-bound MOPr, the presence of a sodium ion did disrupt the norbuprenorphine-bound MOPr, causing it to occupy a more inactive conformation. Other MD studies that started with a sodium ion occupying the allosteric site of the active-like adenosine A<sub>2A</sub> receptor have observed either the sodium leaving the binding pocket or the sodium ion remaining bound and the GPCR adopting an inactive conformation whilst agonist binding is destabilised [49]. Here, the sodium ion did not leave the receptor pore, but the bound ligand and MOPr adopted inactive conformations. This perhaps reflects the relatively short simulation time and that the simulations were started from an already inactive receptor structure, therefore favouring retention of the sodium ion in the allosteric pocket and destabilisation of the agonist binding pocket.

We propose that the distinct receptor conformations captured by the PCA reflect the differing ligand efficacies at the MOPr. Although the BRET experiments suggested that norbuprenorphine may display some bias towards arrestin recruitment, this is yet to be validated in further experiments, and so, the ability to discriminate between an active MOPr conformation and an arrestin-biased conformation by MD simula-

tions is yet to be achieved. In order to characterise receptor conformations that favour G protein or arrestin signalling, a larger set of structurally diverse test compounds, some displaying a strong bias for G protein or arrestin signalling, would be required.

In conclusion, this study has identified molecular differences between structurally related MOPr ligands that correlate with their different intrinsic agonist efficacies. MD simulations showed the high efficacy agonist norbuprenorphine favouring an alternative position in the binding pocket to the low efficacy agonist buprenorphine and the antagonist diprenorphine, without the overlap of the morphinan scaffold. This different pose allowed norbuprenorphine to interact with the W293<sup>6,48</sup> toggle switch, important for GPCR activation and part of the allosteric sodium site. Importantly, the MOPr TMs occupy distinct sets of conformations with a different ligand bound. Together, these results suggest that small changes in the ligand binding pose and ligand-residue interactions lead to global conformational changes in the MOPr helices and induce different receptor conformations. These alternative helical conformations identified in this MD study may confer different abilities of MOPr to activate intracellular signalling partners.

## Materials and Methods

### Cell culture and transfection

HEK 293 cells were cultured at 37 °C in Dulbecco's modified Eagle's medium (DMEM) supplemented with 10% foetal bovine serum and penicillin/streptomycin. Cells were seeded onto 10-cm dishes and grown to 80% confluence before transfection. Cells were transfected with a 1:1 ratio of rat MOPr conjugated to YFP and arrestin tagged with Rluc or with a 1:1:1 ratio of HA-tagged rat MOPr, Gai-RlucII, and G $\beta$  $\gamma$ -GFP, 24 h before assay, using jetPEI DNA transfection reagent (Polyplus).

### BRET assay

Immediately prior to assay, cells were resuspended in clear DMEM and then transferred to a 96-well plate at 90  $\mu$ l per well. DAMGO, buprenorphine, and norbuprenorphine dissolved in water; diprenorphine dissolved in DMSO; and coelenterazine h and coelenterazine 400a dissolved in methanol were diluted in DMEM media to the required concentration. The final DMSO concentration for diprenorphine and controls was 0.01%. The BRET assay was performed on the FLUOstar Omega microplate reader. Drugs and coelenterazine were added at time 0, and the luminescence was measured over 2 min (G protein activation) or 10 min (arrestin recruitment). The ratio

???

of the light emitted by YFP or GFP to the light emitted by Rluc was used to calculate the BRET ratio. To determine whether diprenorphine can antagonise the DAMGO response, we incubated the cells with 1  $\mu$ M diprenorphine for 10 min, prior to the addition of 10  $\mu$ M DAMGO, and the assay was performed as described above. All treatments were performed in duplicate, and the average response was taken. The assay was repeated in 3–6 independent experiments. Data were expressed as the percentage increase (arrestin recruitment) or decrease (G protein activation) in the BRET ratio from control cells treated with media or media +0.01% DMSO, and analyses and curve fitting were performed in GraphPad Prism version 7. All ligands were compared to DAMGO as the standard high efficacy agonist at MOPr.

### System preparation for MD

The X-ray crystal structure of antagonist-bound MOPr (PDB: 4DKL) [31] was obtained from the Protein Data Bank and prepared in Insight II. Ligands and the T4 lysozyme were removed, and a loop search was performed to find a homologous loop to model in the missing intracellular loop 3. A loop was selected by visual inspection and the residues changed to the correct mouse MOPr sequence (Fig. S6). The side chains were inspected for clashes and bonds rotated where necessary. The receptor was embedded in a POPC:POPE:cholesterol lipid bilayer at a 5:5:1 ratio using the replacement method, and the simulation box (initial dimensions: 90, 110, 90 Å) solvated with TIP3P water and 0.15 M NaCl using the CHARMM-GUI software [50]. The antagonist  $\beta$ -FNA shares a morphinan scaffold with buprenorphine, norbuprenorphine, and diprenorphine. The binding pose of  $\beta$ -FNA in the crystal structure was used as a template to determine the initial orientation of the ligands for MD simulation. Ligands were parameterised using Antechamber and the general Amber force field [51]. All ligands were protonated at the amine to allow interaction with D147<sup>3,32</sup>. Amber parameter topology and coordinate files were prepared in LEaP.

### MD simulations and analysis

Structures were minimised over 10,000 steps; then, the system was heated under constant volume and pressure with lipids restrained, from 0 K to 100 K over 5 ps, and then from 100 K to 310 K over 100 ps. We performed 10 rounds of 500-ps equilibration under constant pressure to equilibrate the periodic box dimensions. Each simulation was run for 125 ns under the Amber ff14SB and Lipid14 force fields [52,53]. Temperature and pressure were controlled using the Langevin thermostat and the anisotropic Berendsen barostat, with a 2-fs time step and trajectories written every 100 ps. Simulations were

run for a total of 1  $\mu$ s for each receptor–ligand complex in a series of 8  $\times$  125 ns parallel steps, with newly minimised structures and new random velocities for each simulation, under both cMD and aMD [30]. aMD uses an external boost potential to accelerate conformational changes, allowing for increased sampling over the same amount of computational time as cMD. This technique allows protein conformational changes to be investigated, which would otherwise not be accessible over the short computing time available. Parameters for the aMD were calculated as described in Kappel *et al.* [54]. Trajectories were visualised in VMD, and the analysis was performed using cpptraj [55]. Trajectories were aligned to a set of “core” residues that showed the least amount of movement across the simulations (Fig. S6a) to avoid including general translation and rotation of the protein in the analysis, before RMSD and PCA calculations were performed. The covariance matrix was calculated and diagonalised using cpptraj, and the PCs were obtained by mapping the three-dimensional Cartesian coordinates of the alpha carbons of the TMs of all trajectories (Fig. S6b). Each frame of the simulated trajectories was mapped onto PC1 and PC2 to produce a plot visualising the conformational space occupied by the receptor at each time point. Images of ligand binding poses and side-chain orientations were prepared in Chimera [56].

### Simulations with an allosteric sodium ion

Simulations were also performed with MOPr in the absence of any ligand. During these unliganded simulations, a sodium ion was observed to enter the receptor pore from the extracellular space and occupy the allosteric sodium site (data not shown). The position of this sodium ion was in agreement with the published high-resolution structure of the antagonist-bound  $\delta$ -opioid receptor [19]. The coordinates of this allosteric sodium ion in the unliganded simulation were used to place a sodium ion into the receptor pore of MOPr bound to buprenorphine or norbuprenorphine. Two independent 125ns simulations were run, as described above, for each ligand, under both aMD and cMD simulations, giving a total of 500 ns of trajectory data for each ligand–sodium complex.

has been confirmed by multiple studies.

---

---

### Acknowledgements

This work was supported by a Biotechnology and Biological Sciences Research Council (BBSRC) studentship awarded to K.J.S. under the South West Biosciences (SWBio) DTP scheme (Grant BB/J014400/1), and carried out using the computational facilities of the Advanced Computing

Research Centre, University of Bristol – <http://www.bris.ac.uk/acrc/>. We thank Dr. Michel Bouvier, University of Montreal, for the gift of the G protein BRET constructs (NB Domain Therapeutics is the holder of the license for all commercial use of the constructs), and Dr. Nick Holliday, University of Nottingham, for the arrestin-3 BRET construct.

## Appendix A. Supplementary Data

Supplementary data to this article can be found online at <http://dx.doi.org/10.1016/j.jmb.2017.05.009>.

Received 11 January 2017;

Received in revised form 7 May 2017;

Accepted 8 May 2017

Available online 11 May 2017

### Keywords:

G protein-coupled receptor;  
 $\mu$ -opioid receptor;  
molecular dynamics;  
buprenorphine

### Abbreviations used:

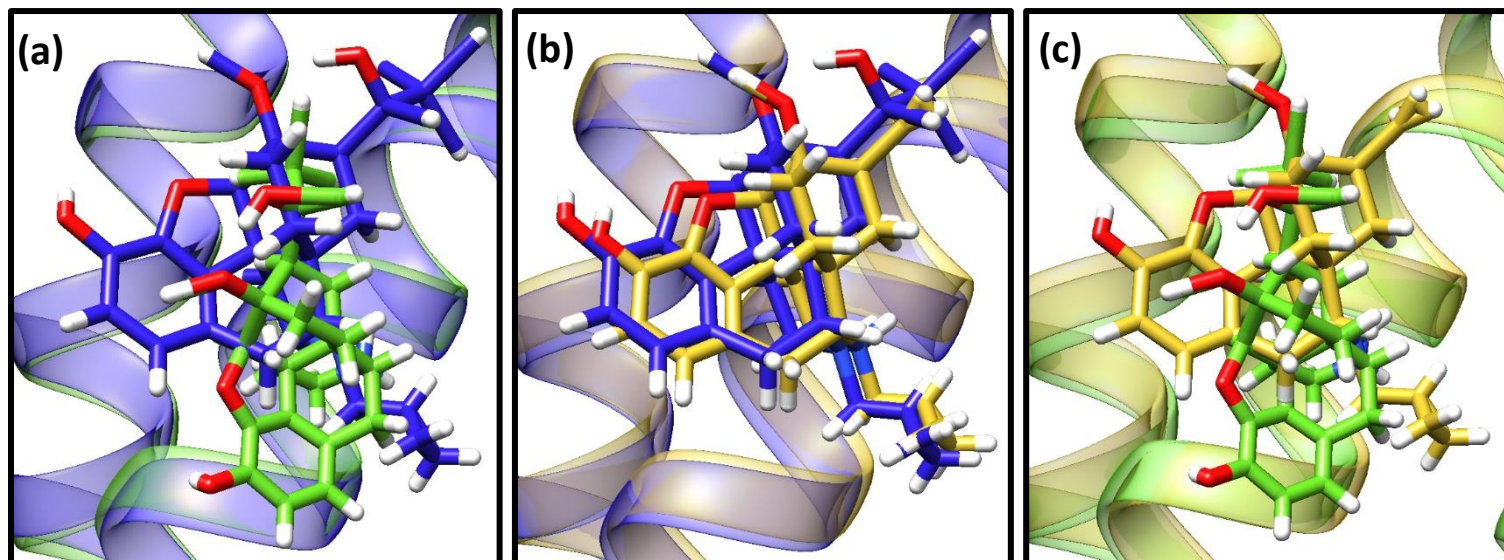
MOPr,  $\mu$ -opioid receptor; GPCR, G protein-coupled receptor; TM, transmembrane domain; BRET, bioluminescence resonance energy transfer; MD, molecular dynamics; HEK 293, human embryonic kidney 293; Rluc, renilla luciferase; GFP, green fluorescent protein; YFP, yellow fluorescent protein; cMD, conventional MD; aMD, accelerated MD;  $\beta$ -FNA,  $\beta$ -funaltrexamine; PC, principal component; PCA, principal component analysis; DMEM, Dulbecco's modified Eagle's medium.

## References

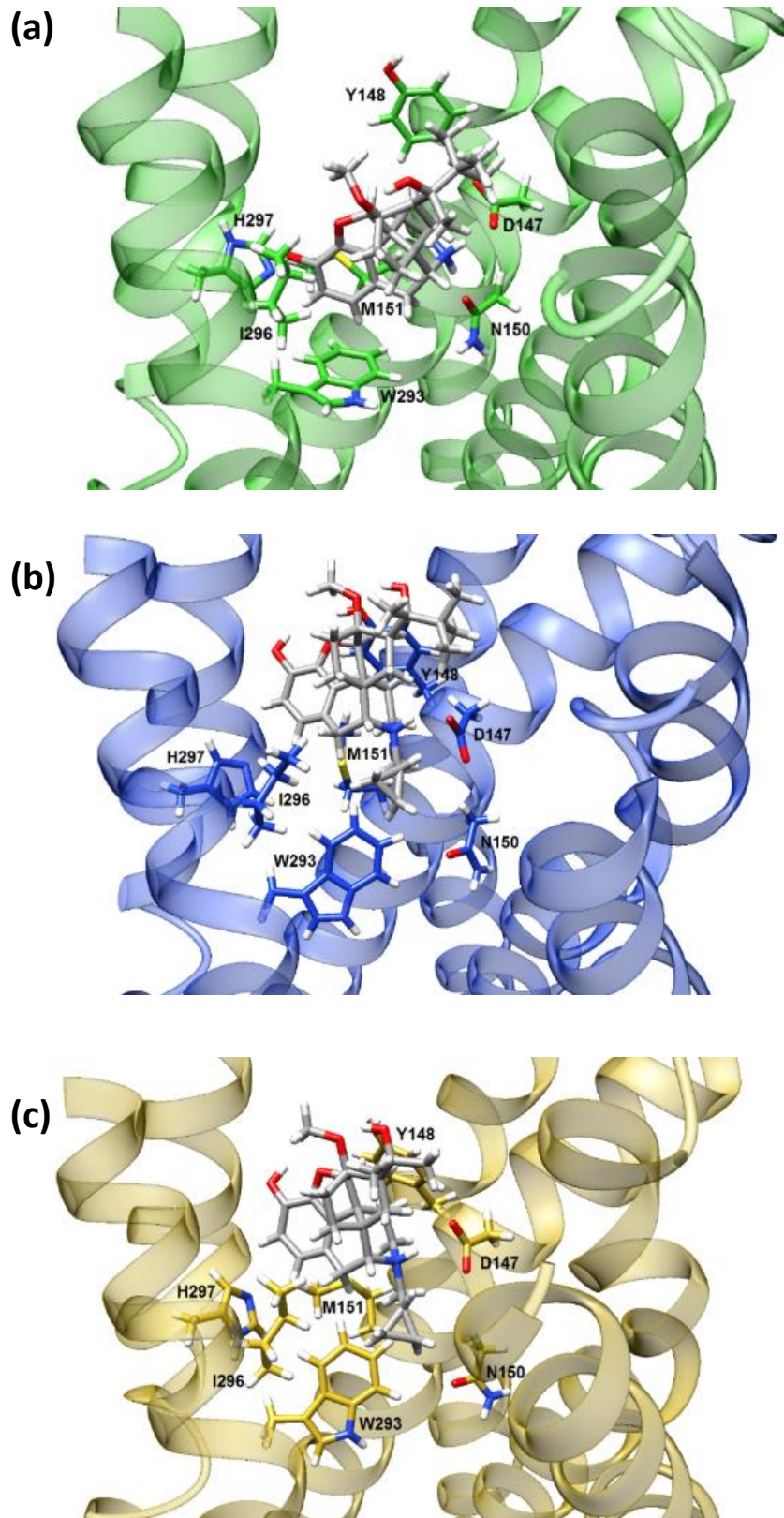
- [1] H.W. Matthes, R. Maldonado, F. Simonin, O. Valverde, S. Slowe, I. Kitchen, et al., Loss of morphine-induced analgesia, reward effect and withdrawal symptoms in mice lacking the  $\mu$ -opioid-receptor gene, *Nature* 383 (1996) 819–823.
- [2] D. Zhang, Q. Zhao, B. Wu, Structural studies of G protein-coupled receptors, *Mol. Cells* 38 (2015) 836–842.
- [3] V. Katritch, V. Cherezov, R.C. Stevens, Structure-function of the G-protein-coupled receptor superfamily, *Annu. Rev. Pharmacol.* 53 (2013) 531–556.
- [4] J.A.R. Dalton, I. Lans, J. Giraldo, Quantifying conformational changes in GPCRs: glimpse of a common functional mechanism, *BMC Bioinformatics* 16 (2015) 124.
- [5] P. Huang, J. Li, C. Chen, I. Visiers, H. Weinstein, L.Y. Liu-Chen, Functional role of a conserved motif in TM6 of the rat  $\mu$  opioid receptor: constitutively active and inactive receptors result from substitutions of Thr6.34(279) with Lys and Asp, *Biochemistry* 40 (2001) 13,501–13,509.
- [6] W. Huang, A. Manglik, A.J. Venkatakrishnan, T. Laeremans, E.N. Feinberg, A.L. Sanborn, et al., Structural insights into  $\mu$ -opioid receptor activation, *Nature* 524 (2015) 315–321.
- [7] R. Sounier, C. Mas, J. Steyaert, T. Laeremans, A. Manglik, W. Huang, et al., Propagation of conformational changes during  $\mu$ -opioid receptor activation, *Nature* 524 (2015) 375–378.
- [8] Y. Kang, X.E. Zhou, X. Gao, Y. He, W. Liu, A. Ishchenko, et al., Crystal structure of rhodopsin bound to arrestin by femtosecond X-ray laser, *Nature* 523 (2015) 561–567.
- [9] B.G. Tehan, A. Bortolato, F.E. Blaney, M.P. Weir, J.S. Mason, Unifying family A GPCR theories of activation, *Pharmacol. Ther.* 143 (2014) 51–60.
- [10] R.O. Dror, D.H. Arlow, P. Maragakis, T.J. Mildorf, A.C. Pan, H. Xu, et al., Activation mechanism of the  $\beta$ 2-adrenergic receptor, *Proc. Natl. Acad. Sci. U. S. A.* 108 (2011) 18,684–18,689.
- [11] D. Wootten, C.A. Reynolds, C. Koole, K.J. Smith, J.C. Mobarec, J. Simms, et al., A hydrogen-bonded polar network in the core of the glucagon-like peptide-1 receptor is a fulcrum for biased agonism: lessons from class B crystal structures, *Mol. Pharmacol.* 89 (2016) 335–347.
- [12] W. Liu, E. Chun, A.A. Thompson, P. Chubukov, F. Xu, V. Katritch, et al., Structural basis for allosteric regulation of GPCRs by sodium ions, *Science* 337 (2012) 232–236.
- [13] D.E. Selley, C.C. Cao, Q. Liu, S.R. Childers, Effects of sodium on agonist efficacy for G-protein activation in  $\mu$ -opioid receptor-transfected CHO cells and rat thalamus, *Br. J. Pharmacol.* 130 (2000) 987–996.
- [14] V. Katritch, G. Fenalti, E.E. Abola, B.L. Roth, V. Cherezov, R.C. Stevens, Allosteric sodium in class A GPCR signaling, *Trends Biochem. Sci.* 39 (2014) 233–244.
- [15] Y. Miao, A.D. Caliman, J.A. McCammon, Allosteric effects of sodium ion binding on activation of the M3 muscarinic G-protein-coupled receptor, *Biophys. J.* 108 (2015) 1796–1806.
- [16] Y. Shang, V. LeRouzic, S. Schneider, P. Bisignano, G.W. Pasternak, M. Filizola, Mechanistic insights into the allosteric modulation of opioid receptors by sodium ions, *Biochemistry* 53 (2014) 5140–5149.
- [17] C.B. Pert, S.H. Snyder, Opiate receptor binding of agonists and antagonists affected differentially by sodium, *Mol. Pharmacol.* 10 (1974) 868–879.
- [18] S. Yuan, H. Vogel, S. Filipek, The role of water and sodium ions in the activation of the  $\mu$ -opioid receptor, *Angew. Chem. Int. Ed. Engl.* 52 (2013) 10,112–10,115.
- [19] G. Fenalti, P.M. Giguere, V. Katritch, X.P. Huang, A.A. Thompson, V. Cherezov, et al., Molecular control of  $\delta$ -opioid receptor signalling, *Nature* 506 (2014) 191–196.
- [20] A. Massink, H. Gutierrez-de-Teran, E.B. Lenselink, N.V. Ortiz Zacarias, L. Xia, L.H. Heitman, et al., Sodium ion binding pocket mutations and adenosine A2A receptor function, *Mol. Pharmacol.* 87 (2015) 305–313.
- [21] K.E. Livingston, J.R. Traynor, Disruption of the Na<sup>+</sup> ion binding site as a mechanism for positive allosteric modulation of the  $\mu$ -opioid receptor, *Proc. Natl. Acad. Sci. U. S. A.* 111 (2014) 18,369–18,374.
- [22] L.A. Stoddart, B. Kellam, S.J. Briddon, S.J. Hill, Effect of a toggle switch mutation in TM6 of the human adenosine A(3) receptor on Gi protein-dependent signalling and Gi-independent receptor internalization, *Br. J. Pharmacol.* 171 (2014) 3827–3844.
- [23] H. Zhang, H. Unal, R. Desnoyer, G.W. Han, N. Patel, V. Katritch, et al., Structural basis for ligand recognition and functional selectivity at angiotensin receptor, *J. Biol. Chem.* 290 (2015) 29,127–29,139.
- [24] L. Toll, I.P. Berzetei-Gurske, W.E. Polgar, S.R. Brandt, I.D. Adapa, L. Rodriguez, et al., Standard binding and functional assays related to medications development division testing for potential cocaine and opiate narcotic treatment medications, *NIDA Res. Monogr.* 178 (1998) 440–466.

- [25] P. Huang, G.B. Kehner, A. Cowan, L.Y. Liu-Chen, Comparison of pharmacological activities of buprenorphine and norbuprenorphine: norbuprenorphine is a potent opioid agonist, *J. Pharmacol. Exp. Ther.* 297 (2001) 688–695.
- [26] E.J. Cone, C.W. Gorodetzky, D. Yousefnejad, W.F. Buchwald, R.E. Johnson, The metabolism and excretion of buprenorphine in humans, *Drug Metab. Dispos.* 12 (1984) 577–581.
- [27] J. McPherson, G. Rivero, M. Baptist, J. Llorente, S. Al-Sabah, C. Krasel, et al.,  $\mu$ -opioid receptors: correlation of agonist efficacy for signalling with ability to activate internalization, *Mol. Pharmacol.* 78 (2010) 756–766.
- [28] C. Denis, A. Saulière, S. Galandrin, J.M. Sénard, C. Galés, Probing heterotrimeric G protein activation: applications to biased ligands, *Curr. Pharm. Des.* 18 (2012) 128–144.
- [29] P. Molinari, I. Casella, T. Costa, Functional complementation of high-efficiency resonance energy transfer: a new tool for the study of protein binding interactions in living cells, *Biochem. J.* 409 (2008) 251–261.
- [30] L.C. Pierce, R. Salomon-Ferrer, C. Augusto F de Oliveira, J.A. McCammon, R.C. Walker, Routine access to millisecond time scale events with accelerated molecular dynamics, *J. Chem. Theory Comput.* 8 (2012) 2997–3002.
- [31] A. Manglik, A.C. Kruse, T.S. Kobilka, F.S. Thian, J.M. Mathiesen, R.K. Sunahara, et al., Crystal structure of the  $\mu$ -opioid receptor bound to a morphinan antagonist, *Nature* 485 (2012) 321–326.
- [32] X. Cui, A. Yeliseev, R. Liu, Ligand interaction, binding site and G protein activation of the  $\mu$  opioid receptor, *Eur. J. Pharmacol.* 702 (2013) 309–315.
- [33] J.A. Ballesteros, H. Weinstein, Integrated methods for the construction of three-dimensional models and computational probing of structure-function relations in G protein-coupled receptors, *Methods Neurosci.* 25 (1995) 366–428.
- [34] T. Kaserer, A. Lantero, H. Schmidhammer, M. Spetea, D. Schuster,  $\mu$  opioid receptor: novel antagonists and structural modeling, *Sci. Rep.* 6 (2016) 21,548.
- [35] M.S. Virk, S. Arttamangkul, W.T. Birdsong, J.T. Williams, Buprenorphine is a weak partial agonist that inhibits opioid receptor desensitization, *J. Neurosci.* 29 (2009) 7341–7348.
- [36] A. Amadei, A.B. Linssen, H.J. Berendsen, Essential dynamics of proteins, *Proteins* 17 (1993) 412–425.
- [37] A. Knapman, M. Santiago, M. Connor, A6V polymorphism of the human  $\mu$ -opioid receptor decreases signalling of morphine and endogenous opioids *in vitro*, *Br. J. Pharmacol.* 172 (2015) 2258–2272.
- [38] H.C.S. Chan, S. Filipek, S. Yuan, The principles of ligand specificity on  $\beta$ 2-adrenergic receptor, *Sci. Rep.* 6 (2016) 34,736.
- [39] J. Shim, A. Coop, A.D. MacKerell Jr., Consensus 3D model of  $\mu$ -opioid receptor ligand efficacy based on a quantitative conformationally sampled pharmacophore, *J. Phys. Chem. B* 115 (2011) 7487–7496.
- [40] J. Shim, A. Coop, A.D. MacKerell Jr., Molecular details of the activation of the  $\mu$  opioid receptor, *J. Phys. Chem. B* 117 (2013) 7907–7917.
- [41] R. Singh, D.P. Hurst, J. Barnett-Norris, D.L. Lynch, P.H. Reggio, F. Guarnieri, Activation of the cannabinoid CB1 receptor may involve a W6.48/F3.36 rotamer toggle switch, *J. Pept. Res.* 60 (2002) 357–370.
- [42] S.D. McAllister, G. Rizvi, S. Anavi-Goffer, D.P. Hurst, J. Barnett-Norris, D.L. Lynch, et al., An aromatic microdomain at the cannabinoid CB1 receptor constitutes an agonist/inverse agonist binding region, *J. Med. Chem.* 46 (2003) 5139–5152.
- [43] J. Wess, S. Nanavati, Z. Vogel, R. Maggio, Functional role of proline and tryptophan residues highly conserved among G protein-coupled receptors studied by mutational analysis of the M3 muscarinic receptor, *EMBO J.* 12 (1993) 331–338.
- [44] B. Holst, R. Nygaard, L. Valentin-Hansen, A. Bach, M.S. Engelstoft, P.S. Petersen, et al., A conserved aromatic lock for the tryptophan rotameric switch in TM-VI of seven-transmembrane receptors, *J. Biol. Chem.* 285 (2010) 3973–3985.
- [45] L. Valentin-Hansen, T.M. Frimurer, J. Mokrosinski, N.D. Holliday, T.W. Schwartz, Biased Gs *versus* Gq proteins and  $\beta$ -arrestin signaling in the NK1 receptor determined by interactions in the water hydrogen bond network, *J. Biol. Chem.* 290 (2015) 24,495–24,508.
- [46] A. Manglik, H. Lin, D.K. Aryal, J.D. McCorvy, D. Dengler, G. Corder, et al., Structure-based discovery of opioid analgesics with reduced side effects, *Nature* 537 (2016) 185–190.
- [47] X. Cong, P. Campomanes, A. Kless, I. Schapitz, M. Wagener, T. Koch, et al., Structural determinants for the binding of morphinan agonists to the  $\mu$ -opioid receptor, *PLoS One* 10 (2015) e0135998.
- [48] S. Schneider, D. Provasi, M. Filizola, How olliceridine (TRV-130) binds and stabilizes a  $\mu$ -opioid receptor conformational state that selectively triggers G protein-signaling pathways, *Biochemistry* 55 (2016) 6456–6466.
- [49] H. Gutierrez-de-Teran, A. Massink, D. Rodriguez, W. Liu, G.W. Han, J.S. Joseph, et al., The role of a sodium ion binding site in the allosteric modulation of the  $\alpha$ (2A) adenosine G protein-coupled receptor, *Structure* 21 (2013) 2175–2185.
- [50] S. Jo, T. Kim, V.G. Iyer, W. Im, CHARMM-GUI: a web-based graphical user interface for CHARMM, *J. Comput. Chem.* 29 (2008) 1859–1865.
- [51] J. Wang, R.M. Wolf, J.W. Caldwell, P.A. Kollman, D.A. Case, Development and testing of a general Amber force field, *J. Comput. Chem.* 25 (2004) 1157–1174.
- [52] J.A. Maier, C. Martinez, K. Kasavajhala, L. Wickstrom, K.E. Hauser, C. Simmerling, ff14SB: improving the accuracy of protein side chain and backbone parameters from ff99SB, *J. Chem. Theory Comput.* 11 (2015) 3696–3713.
- [53] C.J. Dickson, B.D. Madej, A.A. Skjevik, R.M. Betz, K. Teigen, I.R. Gould, et al., Lipid14: the Amber lipid force field, *J. Chem. Theory Comput.* 10 (2014) 865–879.
- [54] K. Kappel, Y. Miao, J.A. McCammon, Accelerated molecular dynamics simulations of ligand binding to a muscarinic G-protein-coupled receptor, *Q. Rev. Biophys.* 48 (2015) 479–487.
- [55] D.R. Roe, T.E. Cheatham III, PTRAJ and CPPTRAJ: software for processing and analysis of molecular dynamics trajectory data, *J. Chem. Theory Comput.* 9 (2013) 3084–3095.
- [56] E.F. Pettersen, T.D. Goddard, C.C. Huang, G.S. Couch, D.M. Greenblatt, E.C. Meng, et al., UCSF chimera—a visualization system for exploratory research and analysis, *J. Comput. Chem.* 25 (2004) 1605–1612.

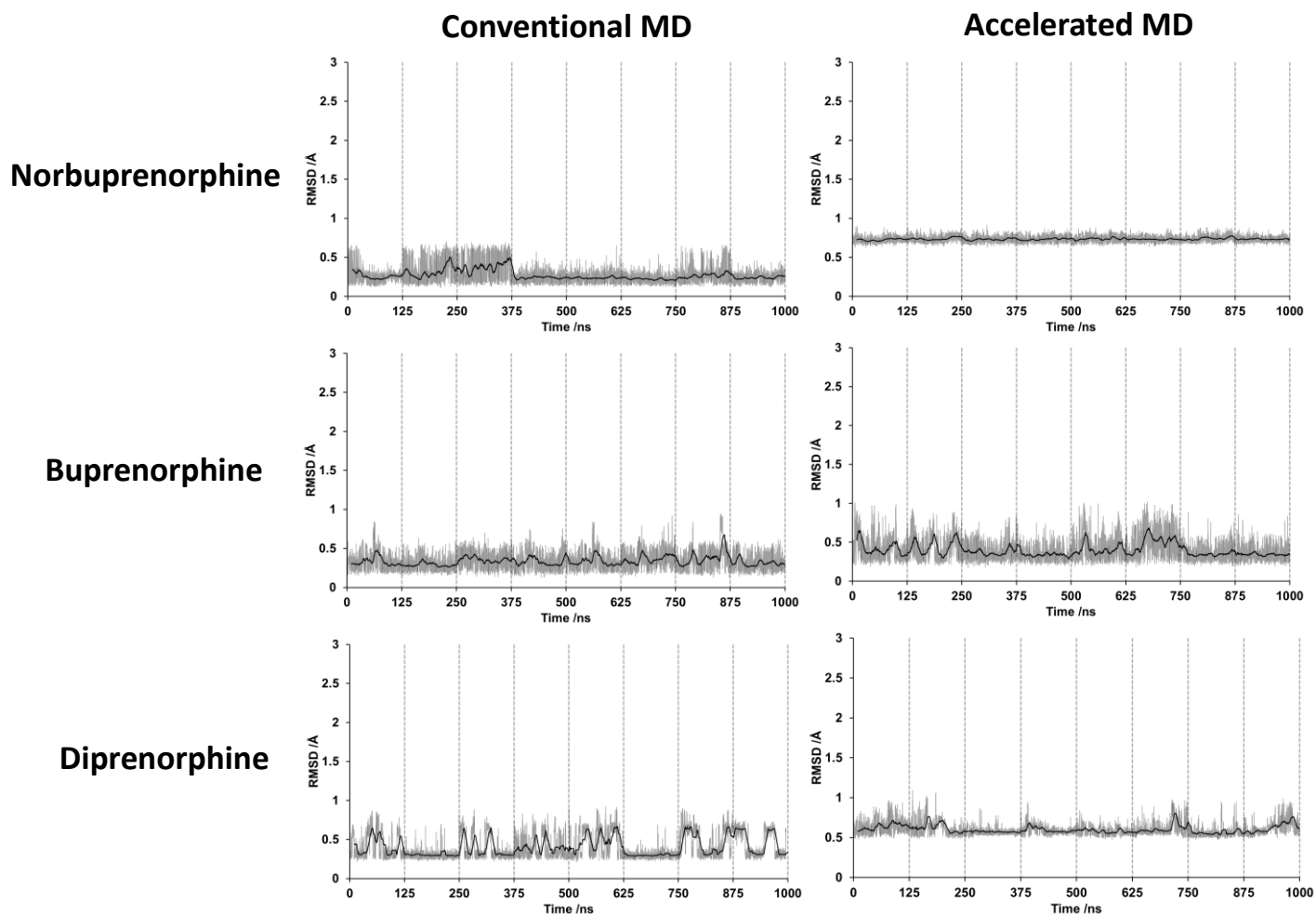
## Supplementary figures



**Supplementary Fig. 1. Ligand binding poses.** Overlay of the average binding poses of MOPr ligands from 1  $\mu$ s of accelerated MD simulations. Buprenorphine (blue) and diprenorphine (yellow) adopt a position higher in the binding pocket than norbuprenorphine (green).

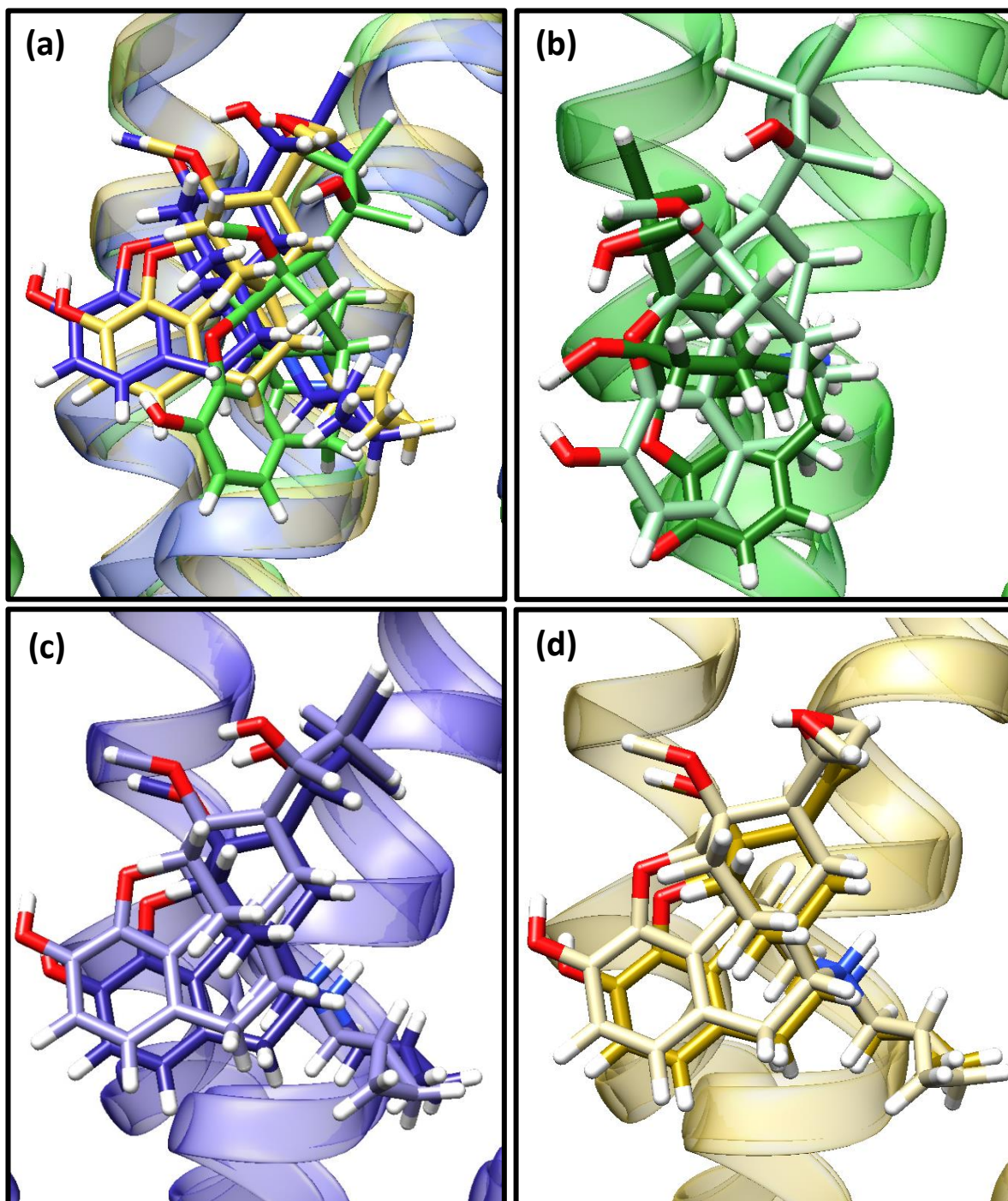


**Supplementary Fig. 2. Ligand binding poses and key residues.** Representative snapshots of the binding poses of: (a) norbuprenorphine; (b) buprenorphine; (c) diprenorphine. Structures are viewed looking through the lipid bilayer at the side of the receptor. Key interacting residues forming the ligand binding pocket are depicted.



**Supplementary Fig. 3. RMSD plots show ligand binding poses are stable.**

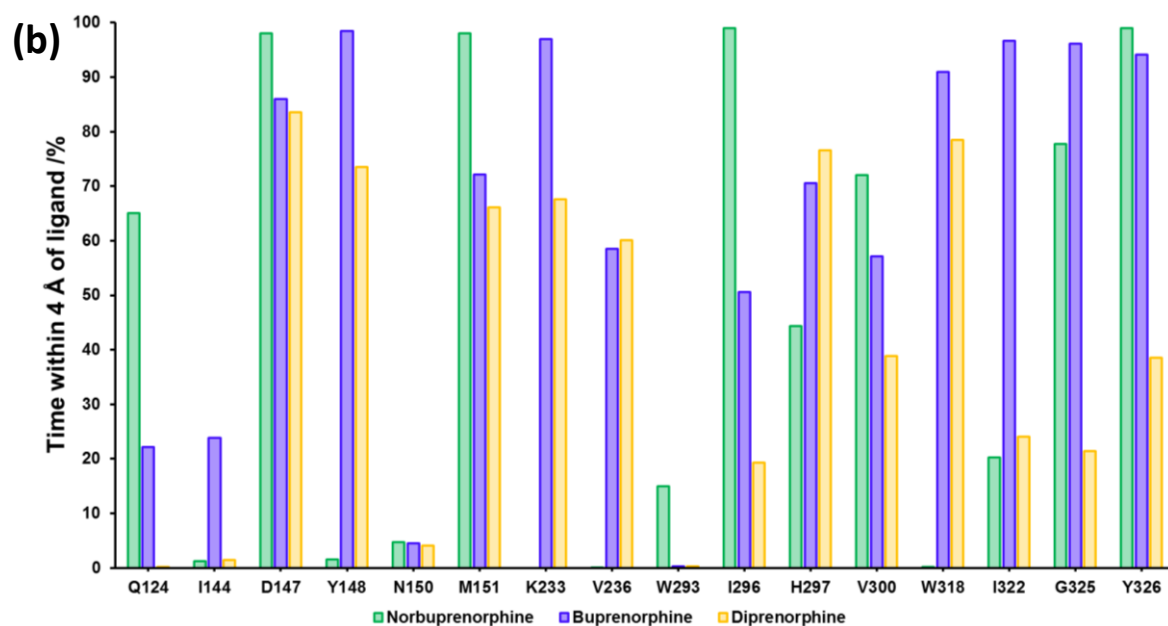
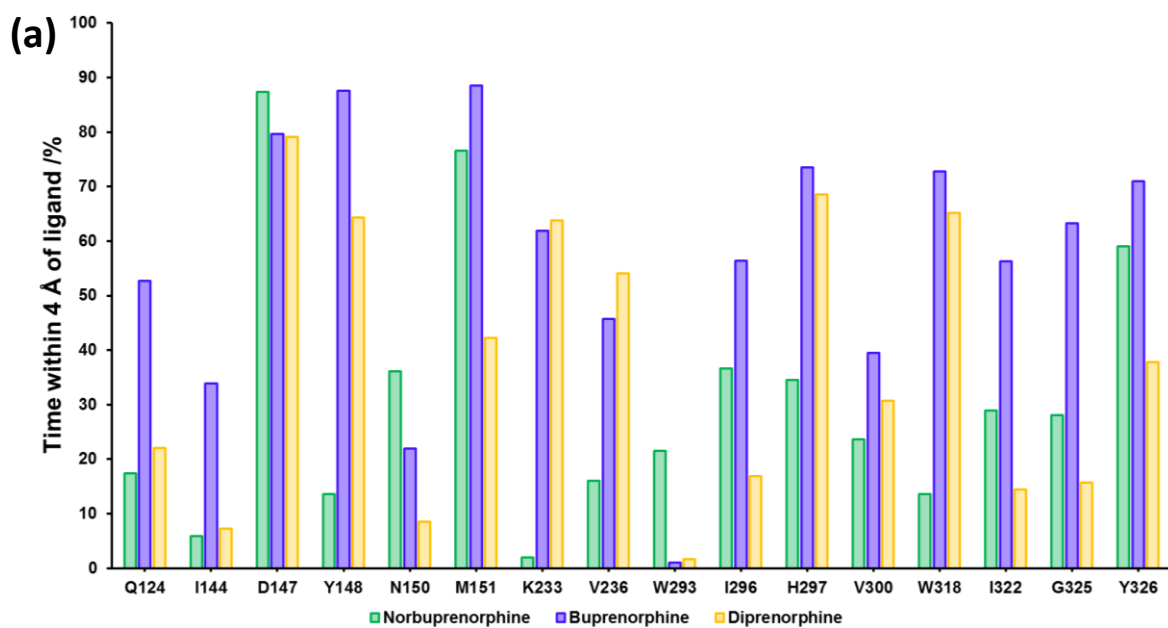
RMSD plots of the heavy atoms of each ligand compared to each ligand's average binding pose. The binding positions are stable over 1  $\mu$ s of cMD and aMD.



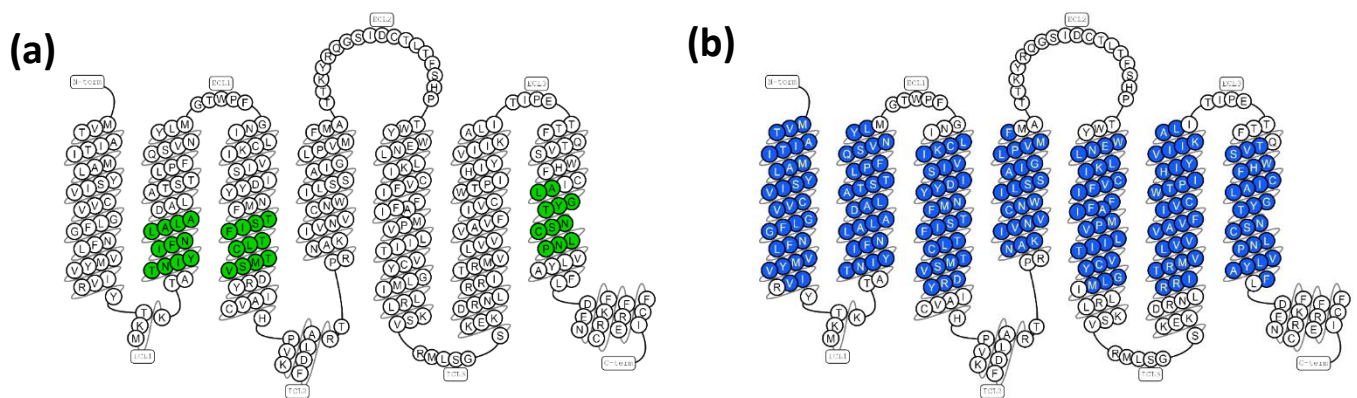
**Supplementary Fig. 4. The average binding poses for aMD and cMD are very similar.**

(a) Overlay of the average binding poses for each ligand from 1  $\mu$ s cMD simulations. (b) Average poses for norbuprenorphine from the cMD (light green) and aMD (dark green) simulations. (c) Average binding poses for buprenorphine from cMD (light blue) and aMD (dark blue) simulations. (d) Average poses for diprenorphine from the cMD (light yellow) and aMD (dark yellow) simulations.



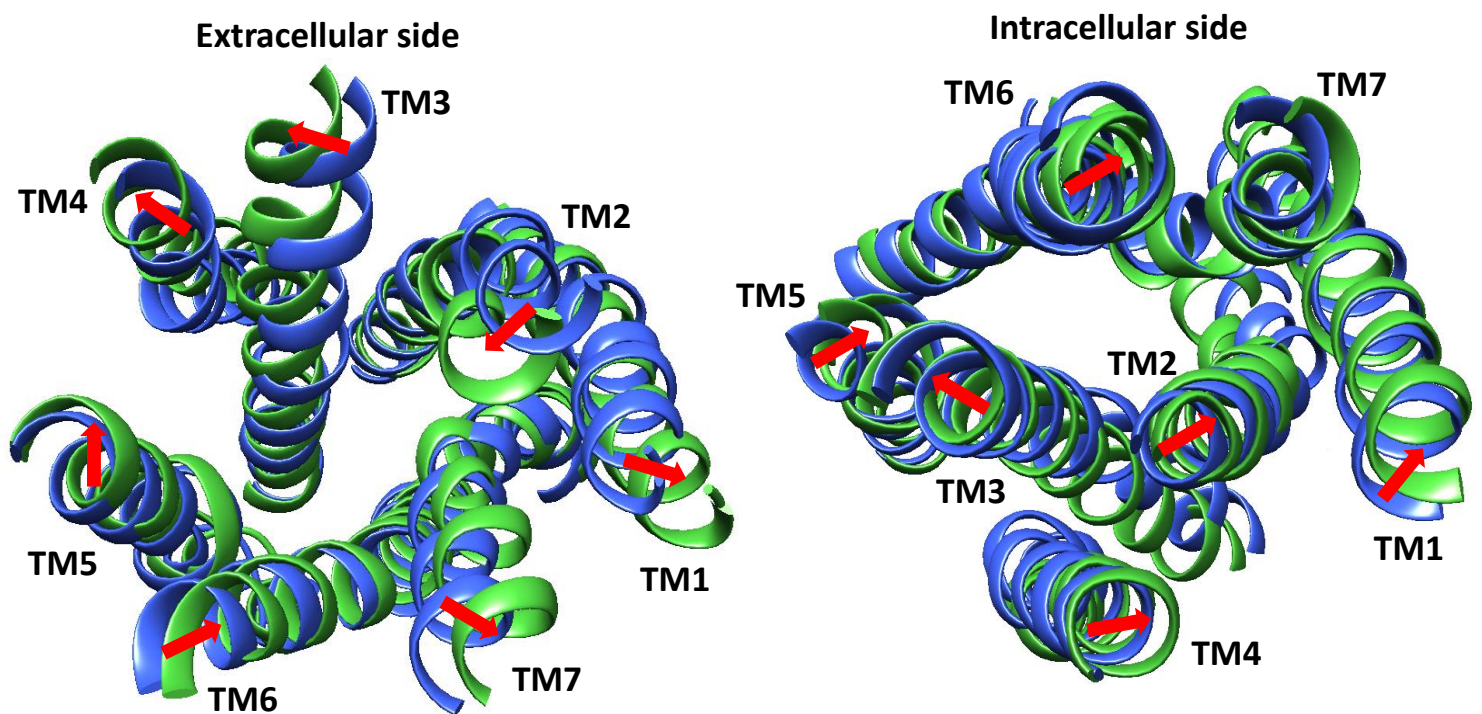


**Supplementary Fig. 5. Ligand-residue interactions as a percentage of simulation time.** Percentage of the simulation time that residues are found within 4 Angstroms of the bound ligand for (a) 1  $\mu$ s of accelerated MD and (b) 1  $\mu$ s of conventional MD.



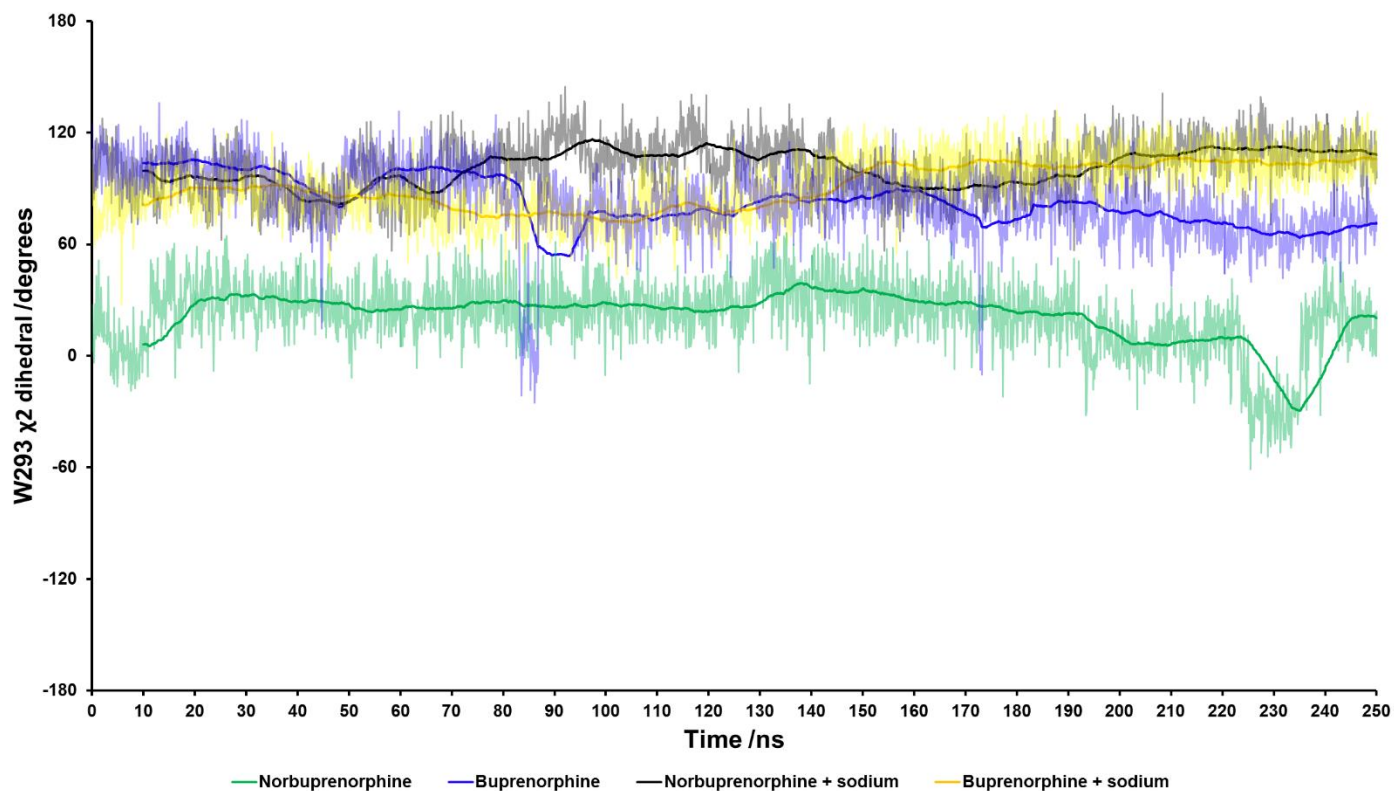
**Supplementary Fig. 6. Snake plots of the murine MOPr sequence used in the MD simulations.**

(a) The core residues to which the trajectories are aligned prior to PCA are shown in green. (b) The transmembrane domain regions for the PCA are shown in blue.

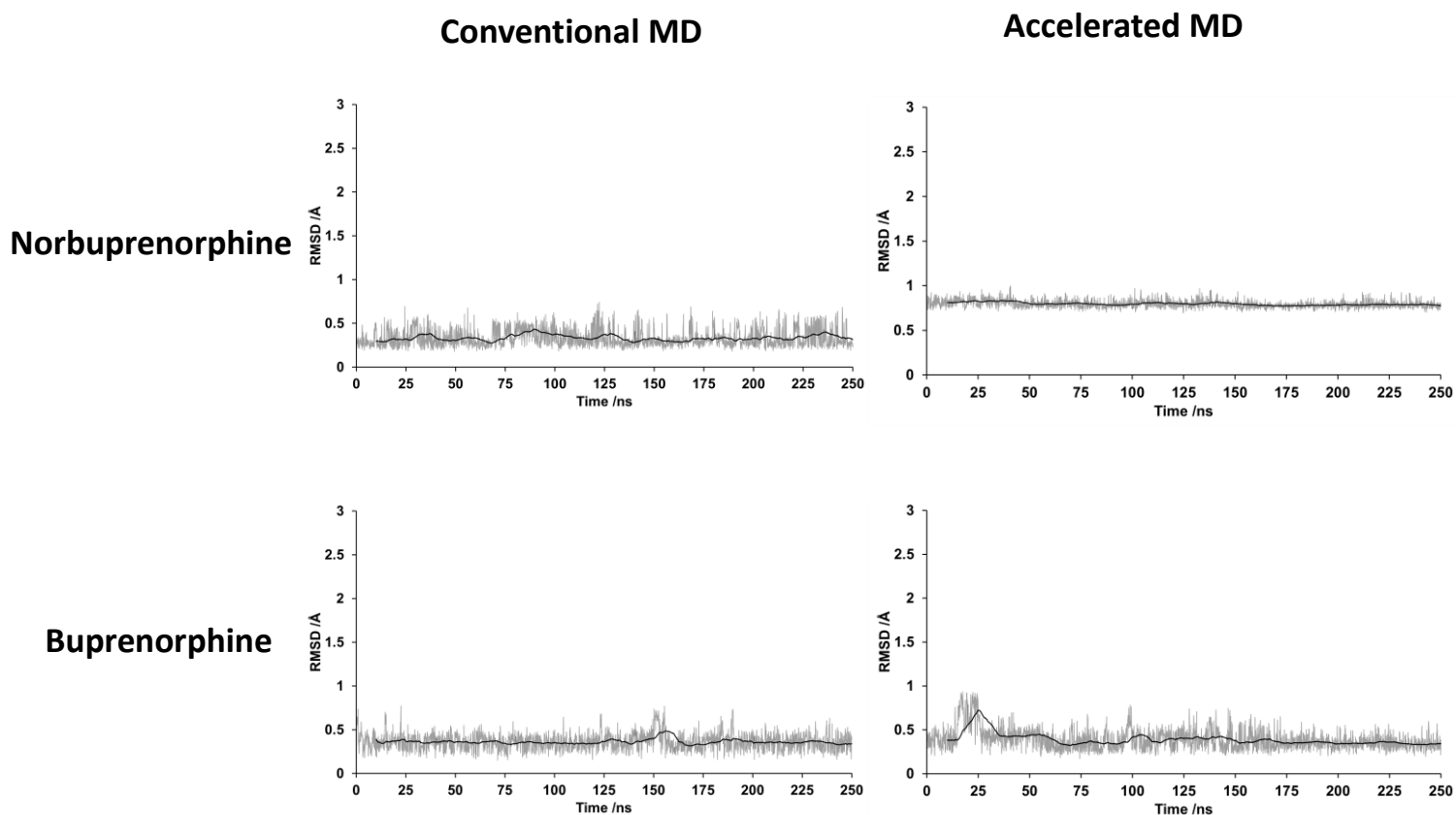


**Supplementary Fig. 7. Structures extracted from the PCA plot for 1  $\mu$ s cMD simulations.**

Red arrows indicate shifts of the helices between the structure extracted from the buprenorphine-bound cluster (blue) and the structure extracted from the norbuprenorphine-bound cluster (green).



**Supplementary Fig. 8. W293<sup>6.48</sup> conformation in the presence and absence of an allosteric sodium.** Rotamer angle of W293<sup>6.48</sup> over 250 ns conventional MD with norbuprenorphine or buprenorphine bound, in the presence or absence of an allosteric sodium ion. Presence of an allosteric sodium causes W293<sup>6.48</sup> to adopt a similar rotamer angle to the buprenorphine- and diprenorphine-bound simulations. Each dataset is plotted as raw data and a running average (solid lines).



**Supplementary Fig. 9. RMSD plots show ligand binding poses in the presence of an allosteric sodium ion are stable.**

RMSD plots of the heavy atoms of each ligand compared to each ligand's average binding pose. The binding positions are stable over 250 ns of cMD and aMD.